

Skew Probabilistic Neural Networks for Learning from Imbalanced Data

Shraddha M. Naik^{a,b}, Tanujit Chakraborty^{1b}, Abdenour Hadid^b, Bibhas Chakraborty^{c,d,e}

^aManipal Academy of Higher Education, Manipal, Karnataka, India

^bSorbonne Center for Artificial Intelligence, Sorbonne University Abu Dhabi, UAE

^cCentre for Quantitative Medicine, Duke-NUS Medical School, National University of Singapore, Singapore

^dDepartment of Statistics and Data Science, National University of Singapore, Singapore

^eDepartment of Biostatistics and Bioinformatics, Duke University, USA

Abstract

Real-world datasets often exhibit imbalanced data distribution, where certain class levels are severely underrepresented. In such cases, traditional pattern classifiers have shown a bias towards the majority class, impeding accurate predictions for the minority class. This paper introduces an imbalanced data-oriented approach using probabilistic neural networks (PNNs) with a skew normal probability kernel to address this major challenge. PNNs are known for providing probabilistic outputs, enabling quantification of prediction confidence and uncertainty handling. By leveraging the skew normal distribution, which offers increased flexibility, particularly for imbalanced and non-symmetric data, our proposed Skew Probabilistic Neural Networks (SkewPNNs) can better represent underlying class densities. To optimize the performance of the proposed approach on imbalanced datasets, hyperparameter fine-tuning is imperative. To this end, we employ a population-based heuristic algorithm, Bat optimization algorithms, for effectively exploring the hyperparameter space. We also prove the statistical consistency of the density estimates which suggests that the true distribution will be approached smoothly as the sample size increases. Experimental simulations have been conducted on different synthetic datasets, comparing various benchmark-imbalanced learners. Our real-data analysis shows that SkewPNNs substantially outperform state-of-the-art machine learning methods for both balanced and imbalanced datasets in most experimental settings.

Keywords: Imbalanced Classification, Probabilistic Neural Networks, Skew normal distribution, Bat algorithm, Consistency

1. Introduction

Data imbalance is ubiquitous and inherent in real-world applications, encompassing rare event prediction, medical diagnosis, image classification, customer churn prediction, and fraud detection. Instead of preserving an ideal uniform distribution over each class level, real data often exhibit a skewed distribution [41, 44] where specific target value has significantly fewer observations. This situation is known as the “curse of imbalanced data” problem in the pattern recognition literature [29]. This poses a challenge for conventional classifiers, as they tend to favor the majority class, resulting in higher misclassification rates for minority class examples. Therefore, a diverse

¹Corresponding Author: tanujit.chakraborty@sorbonne.ae

array of approaches has been introduced to address class imbalance. Existing solutions for learning from imbalanced data can be categorized into data-level and algorithmic-level approaches [44].

Data-level approaches primarily focus on balancing the distribution of samples between the majority and minority classes, ultimately creating a harmonized dataset for learning endeavors [9, 34]. Data-level approaches can be broadly categorized into three primary sub-categories: under-sampling, over-sampling, and mixed-sampling. Several under-sampling techniques have been introduced, including modified versions of random sampling [76, 62, 64], clustering-based approaches [72, 66, 28], and evolutionary algorithm-based approaches [77, 78, 32]. Among these, clustering-based methods (e.g., edited nearest neighbor) share a common approach of grouping samples with similar attributes and selecting a specific number from each cluster based on pre-defined rules. On the contrary, evolutionary approaches view under-sampling as an optimization challenge within swarm intelligence search algorithms, to minimize information loss and mitigate prediction bias. Moving on to oversampling methods, these techniques typically involve duplicating existing minority samples or generating new ones based on specific rules to achieve a balance in the number of majority and minority instances. A widely recognized approach in this category is the synthetic minority oversampling technique (SMOTE) [19, 30]. SMOTE achieves this by generating new minority instances close to other existing minority examples through interpolation. However, it is worth noting that SMOTE does not take into account the density of the data, potentially leading to increased overlap between classes. As a response to this limitation, several extensions of SMOTE have been proposed to address this issue, including majority-weighted minority oversampling [10], borderline-SMOTE [37], adaptive synthetic sampling (ADASYN) [40], and convex hull based SMOTE [74]. The mixed-sampling method integrates both under-sampling and over-sampling techniques, effectively mitigating the drawbacks of reduced diversity in the minority class and substantial information loss in the majority class [68, 43]. It is worth noting that Generative Adversarial Networks (GANs) also possess a high capability to generate synthetic data and to enhance the performance of data-driven machine learning models, especially with deep learning [18]. However, data-level approaches are very sensitive to the presence of outliers, and sampling strategies excessively distort the data distribution often resulting in worse performance in real-world scenarios [26].

Algorithm-level techniques encompass the adaptation of established classifiers to enhance their predictive capabilities, particularly with regard to the minority class. Within this domain, an array of strategies has emerged, leveraging well-known classifiers including support vector machines (SVM) [2], nearest neighbor methods [14, 41], as well as decision trees and random forests [56, 17]. Among them, an SVM variant, the near-Bayesian support vector machine (NBSVM) [24] combines the philosophies of decision boundary shift and unequal regularization costs to elevate overall classification accuracy. Notably, SVMs have played a pivotal role in various strategies aimed at improving imbalanced learning scenarios [27, 57, 65, 50]. Notably, among several algorithmic-level methods, the Hellinger distance decision tree (HDDT), employing Hellinger distance as the splitting criterion, is a very prominent algorithm-level technique in the literature [21]. HDDT, alongside its ensemble counterpart Hellinger distance random forest (HDRF) [23] and other extensions [33, 47, 23], adeptly handles both original and imbalanced datasets. However, HDDTs, while robust against class imbalance, may face overfitting due to a lack of pruning [13]. They can also encounter challenges with sticking to local minima and overfitting, particularly with large trees [15]. To avoid

these challenges, Hellinger net (HN) [16] was proposed for tackling data imbalance for software defect prediction problems. However, the computational expenses resulting in HN training pose a real challenge when working with tabular datasets. Also, there is a lack of works on the development of neural network-based algorithmic solutions dealing with tabular datasets in the imbalanced domain.

The advent of artificial neural networks (ANNs) has revolutionized the field of machine learning, providing robust solutions for a wide range of tasks, including classification and regression tasks [25, 1]. Among the various types of ANNs, probabilistic neural networks (PNNs) have gained significant attention due to their distinctive capability of providing probabilistic outputs [60]. This unique feature allows PNNs to not only perform accurate predictions but also quantify the uncertainty associated with each prediction, making them highly valuable in dealing with uncertain real-world scenarios. At the heart of PNNs lies the utilization of a Gaussian kernel density estimation to model the feature vectors of each class in the training data [48]. This non-parametric technique enables the PNNs to estimate the probability density function for each class, thereby facilitating accurate classification. However, despite its effectiveness in certain scenarios, the Gaussian kernel may not always be the optimal choice for real-world imbalanced datasets due to their complexities and uncertainties that cannot be fully captured by a single Gaussian model. In the statistics literature, skew normal distribution is a popular choice for modeling data with non-zero skewness and asymmetric characteristics [36, 5]. The current work introduces a probabilistic neural networks based on the skew normal distribution, that we call SkewPNNs. Our approach involves estimating multiple smoothing parameters through a heuristic bat algorithm, while the skewness parameter is selected from a range of $[-6, 6]$. This method demonstrates exceptional efficacy in handling benchmarked datasets within imbalanced settings and is computationally inexpensive. Furthermore, we theoretically show the consistency of the density estimates in SkewPNNs so that it can classify patterns of data with unknown classes based on the initial set of patterns, the real class of which is known. By shedding light on the benefits of this flexible and adaptable approach, our work lays the foundation for improved decision-making and problem-solving across a wide range of practical applications (both balanced and imbalanced data).

The rest of the paper is structured as follows. Section 2 provides a comprehensive background on skew normal distribution, PNNs, and the bat optimization algorithm. In Section 3, the design of the proposed method is presented, along with the introduction of the fitness function used in the bat algorithm, and its theoretical properties. Experimental results and performance analysis are presented in Section 4. Finally, we conclude the paper with a discussion of the findings and future scope for further research in Section 5.

2. Preliminaries

This section offers a glimpse into the component methods to be used in building the proposed solution. We discuss their mathematical formulations and relevance in this study.

2.1. Skew Normal Distribution

In recent times, the skew normal distribution (both univariate and multivariate cases) [4, 8, 7, 5] has received great importance for modeling skewed data in statistics, econometrics, nonlinear time

series, and finance among many others. The following lemma (for proof, see [5]) played a crucial role in its development:

Lemma 1. *Let $f_0(\cdot)$ be a d -dimensional continuous probability density function (PDF) symmetric around 0. Let G be a one-dimensional cumulative distribution function such that G' (first derivative of G) exists and G' is a density symmetric around 0. Then, $f(x)$ is a density function on \mathbb{R}^d for any (real-valued) odd function $h(x)$ as defined below:*

$$f(x) = 2f_0(x)G\{h(x)\}; \quad x \in \mathbb{R}^d.$$

The above lemma suggests that a symmetric ‘basis’ density f_0 can be manipulated via a ‘perturbation’ function $G\{h(x)\}$ to get a skewed density $f(x)$. Also, the perturbed density will always include a ‘basis’ density. On using $f_0 = \phi(\cdot)$ (density function of the standard normal distribution) and $G = \Phi(\cdot)$ (distribution function of the standard normal distribution) and $h(x) = \alpha x$, where $\alpha \in \mathbb{R}$, we get the skew normal distribution with shape parameter α , denoted by $\text{SN}(\alpha)$, and defined as:

$$f(x, \alpha) = 2\phi(x)\Phi(\alpha x); \quad -\infty < x, \alpha < \infty. \quad (1)$$

For $\alpha = 0$, we obtain the standard normal density. A more general form (also called a three-parameter skew normal distribution) has received considerable attention in the last two decades because of its greater flexibility and applications in various applied fields and is as follows:

$$f(x; \xi, \omega, \alpha) = \frac{2}{\omega} \phi\left(\frac{x - \xi}{\omega}\right) \Phi\left(\frac{\alpha(x - \xi)}{\omega}\right); \quad -\infty < x, \xi, \alpha < \infty, \omega > 0,$$

where ξ is the location parameter, ω is the scale parameter, and α is a skewness (also known as tilt) parameter. Several authors have explored [35, 45, 3, 31] this model to analyze skewed and heavy tail data due to its flexibility. A multivariate extension is straightforward [8] and can be defined as follows: A random vector $\mathbf{X} = (X_1, X_2, \dots, X_d)^T$ is said to follow a d -dimensional multivariate skew normal distribution if it has the following density function:

$$g(\mathbf{x}) = 2\phi_d(\mathbf{x}, \mathbf{\Omega}) \Phi(\alpha^T \mathbf{x}); \quad \mathbf{x} \in \mathbb{R}^d,$$

where $\phi_d(\mathbf{x}, \mathbf{\Omega})$ denotes the PDF of d -dimensional multivariate normal with correlation matrix $\mathbf{\Omega}$ with α is the shape parameter. Inferential statistical properties have been studied and their successful applications are found to analyze several multivariate datasets in various fields, e.g., reliability and survival analysis, due to their flexibility [45].

2.2. Probabilistic Neural Networks (PNNs)

Probabilistic neural networks (PNNs) are a specialized type of single-pass neural network known for their unique architecture. Unlike multi-pass networks, PNNs do not rely on iterative weight adjustments, which simplifies their operation and makes them well-suited for real-time applications [59]. PNNs are particularly notable for their use of Bayesian rules, which enable them to directly estimate posterior probabilities [59, 53]. As a powerful tool for pattern classification tasks, PNNs have garnered significant attention for their capacity to handle uncertainty and offer valuable insights in various real-world applications. This architecture is characterized by four layers, such as

an input layer for processing test patterns, a pattern layer with neurons corresponding to training patterns, a summation layer representing class neurons, and an output layer providing the final classification [59]. PNNs have demonstrated their value across various fields, including medicine, science, business, and industries, owing to their ability to handle real-time data effectively [75].

During training, PNNs utilize the Parzen window, a non-parametric density estimation technique, to approximate the underlying data distribution. For predictions, a winner-takes-all strategy is employed, where the class with the highest probability is selected as the output. This capacity to model the entire PDF empowers PNNs to effectively handle both binary and multi-class classification tasks with remarkable accuracy [48]. In PNNs, the Gaussian distribution is favored for its well-understood properties and straightforward mathematical form. Characterized by mean (μ) and standard deviation (σ), it defines the shape of the distribution. Within PNNs, it is used to estimate class probabilities, associating each training pattern with a Gaussian function centered on its feature values. The spread parameter, determining function width, significantly influences smoothness and generalization. PNNs' effective modeling of data distribution using Gaussian PDF makes them potent for tasks like classification and regression, offering advantages in training, interpretability, and multi-class handling.

Conventional PNNs employ the following mathematical formulation to calculate the PDF of a set of random variables X_1, X_2, \dots, X_n with unknown PDF $g(x)$ is estimated using a family of estimators for each class [59] as

$$f_n(x) = \frac{1}{nh(n)} \sum_{i=1}^n K\left(\frac{x - x_i}{h(n)}\right), \quad (2)$$

where $K(\cdot)$ is a kernel function (discussed below) and the bandwidth $h(n)$ constitutes a sequence of numbers satisfying the condition

$$\lim_{n \rightarrow \infty} h(n) = 0. \quad (3)$$

This process entails the utilization of a non-parametric density estimation technique, such as the Parzen window, to approximate the underlying data distribution for each class (c) individually and given as

$$P_c(x) = \frac{f_n(x)}{\sum f_n(x)}. \quad (4)$$

In vector formulation, for a given new input sample x and a training sample x_i from class c , the Gaussian kernel can be represented as

$$K(x, x_i) = \exp\left(-\frac{1}{2\sigma^2}(x - x_i) \cdot (x - x_i)\right), \quad (5)$$

where σ represents the smoothing parameter, x is the vector representing the input sample, x_i is the vector representing the training sample from class c , and ' \cdot ' denotes the dot product between the two vectors. The Gaussian kernel computes the similarity between the new input sample and each training sample, with higher values indicating stronger similarity. It represents a symmetric, bell-shaped curve centered at 0, with the standard deviation determining the width of the curve. Several notable extensions of PNNs were introduced in the recent literature, namely weighted PNNs [49], self-adaptive PNNs [73], and bat-algorithm-based PNNs [51], among many others which addresses

the complexities of parameter estimation in PNNs. However, none of the above provides a robust solution to the data imbalance problems.

2.3. Optimization of Hyper-parameters via Bat Algorithm (BA)

Bat algorithm (BA) is a meta-heuristic optimization technique inspired by the echolocation behavior observed in bats during their foraging activities [70]. It commences by randomly placing a population of N bats within the search space, with each bat symbolizing a potential solution to the optimization problem at hand [69, 51].

At every iteration t , the velocity ($v_i(t)$) of each bat i is updated based on the disparity between its current position ($\mathcal{X}_i(t)$) and the best solution discovered thus far ($\mathcal{X}_{\text{best}}$). The velocity adjustment is regulated by a fixed frequency f_{min} with a maximum limit of f_{max} and dynamic frequency f_i . The velocity $v_i(t+1)$ at time step $t+1$ is determined as

$$v_i(t+1) = v_i(t) + (\mathcal{X}_{\text{best}} - \mathcal{X}_i(t))f_i, \quad (6)$$

where f_i is computed as $f_i = f_{\text{min}} + (f_{\text{max}} - f_{\text{min}})\beta$, with $\beta \in [0, 1]$. Following the velocity update, the new position ($\mathcal{X}_i(t+1)$) of each bat i is computed by adding the updated velocity to its current position

$$\mathcal{X}_i(t+1) = \mathcal{X}_i(t) + v_i(t+1). \quad (7)$$

Certain bats may engage in local search by exploring neighboring regions. This is achieved by introducing a random displacement controlled by a parameter ϵ , defined as

$$\mathcal{X}_i(t+1) = \mathcal{X}_i(t) + \epsilon A_t, \quad (8)$$

where A_t represents the average loudness, and $\epsilon \in [-1, 1]$. Initially, the positive loudness A_0 is set. To adapt to evolving conditions during the optimization process, the loudness ($A_i(t+1)$) of each bat i diminishes over time to decrease the appeal of a solution. This is updated using a scaling factor λ as $A_i(t+1) = \lambda A_i(t)$. Similarly, the pulse rate ($r_i(t+1)$) governs the likelihood of emitting ultrasound pulses, and is adjusted throughout the optimization process. BA iterates until a specified stopping condition is fulfilled, which could be reaching a maximum iteration count or attaining a predefined level of precision. This iterative process enables the algorithm to effectively navigate the solution space and ultimately converge towards optimal or highly satisfactory solutions. This versatility and effectiveness render the bat algorithm a valuable and potent tool across a range of problem domains and this nature-inspired algorithm combined with PNNs having skew normal kernel is used in this study to address the imbalanced problem.

3. Proposed Method

We introduce the proposed SkewPNNs in this section, followed by Bat algorithm-based Skew-PNNs. Furthermore, we study the consistency of density estimates in SkewPNNs.

3.1. Algorithm 1: SkewPNNs

The PDF for our proposed SkewPNNs of a set of random variables X_1, X_2, \dots, X_n with unknown PDF $g(x)$ is estimated using a family of estimators defined in Eqn. (2) and satisfying condition

stated in Eqn. (3). The skew normal distribution can be used as a kernel function in PNNs for the situation when the data exhibits skewed distributions with a long tail. The skew normal distribution is defined by its location parameter ξ , scale parameter ω , and skewness parameter α . We define the skew normal density to be used in SkewPNNs as follows:

$$f(x; \xi, \omega, \alpha) = \frac{2}{\omega\sqrt{2\pi}} \exp\left(-\frac{(x - \xi)^2}{2\omega^2}\right) \Phi\left\{\alpha\left(\frac{x - \xi}{\omega}\right)\right\}; \quad \xi, x \in (-\infty, \infty), \omega > 0. \quad (9)$$

This kernel function allows the PNNs to effectively handle complex and non-symmetric data distributions, making it a valuable choice for various real-world applications. By considering the skewness of the data, the skew normal kernel enhances the PNN’s ability to provide accurate and probabilistic outputs for classification tasks, particularly when dealing with uncertain and imbalanced datasets. The skew normal-based kernel function without a location parameter is given below

$$K(x, x_i) = \exp\left(-\frac{(x - x_i) \cdot (x - x_i)}{2\omega^2}\right) \Phi\left(\frac{\alpha(x - x_i)}{\omega}\right), \quad (10)$$

where x is the vector representing the new input sample, x_i is the vector representing the training sample from class c , ‘ \cdot ’ denotes the dot product between the two vectors, ω represents the smoothing parameter and Φ denotes the cumulative distribution function (CDF) of the standard normal distribution. The skew normal kernel function now properly accounts for the smoothing parameter ω in the cumulative distribution term, making it a suitable alternative to the Gaussian kernel for handling non-symmetric data distributions in PNNs. The incorporation of skew normal kernels introduces asymmetry to the distribution, enabling a more flexible representation of the data, and these kernels play a pivotal role in PDF computations during both the training and prediction stages of the PNNs model, with the selection of the kernel function being contingent on the data’s characteristics and the specific problem being addressed. Since the Gaussian kernel is a particular case of Eqn. (9), therefore, SkewPNNs can also be useful for classifying balanced datasets as well.

3.2. Algorithm 2: Bat Algorithm-based SkewPNNs

For optimizing the parameters of the skew normal kernel and other hyper-parameters in SkewPNNs, the population-based Bat algorithm is employed. By using the Bat optimization approach, the SkewPNNs can fine-tune their parameters effectively and achieve improved performance, especially when dealing with imbalanced datasets and data with non-symmetric target distributions. The Bat Algorithm’s ability to explore the hyper-parameter space and find suitable solutions contributes to enhancing the SkewPNN’s capability to handle uncertainty and class imbalance, leading to better classification accuracy and robustness in practical applications. The fitness function in the context of the BA is a crucial component that evaluates the quality of candidate solutions (bats) during the optimization process. The primary objective of the fitness function is to quantify how well each bat performs concerning the optimization problem at hand. It provides a numerical measure of the fitness or suitability of a solution, enabling the algorithm to distinguish between better and worse solutions. In case of optimizing the parameters of the skew normal kernel and other hyper-parameters in the SkewPNNs, the fitness function is designed to assess the performance of the SkewPNNs on the given classification task. It typically uses performance metrics such as accuracy, F1-score, or area under the receiver operating characteristic curve (AUC-ROC) to mea-

sure how well the SkewPNNs classify the data. During each iteration of the Bat Algorithm, the fitness function is applied to evaluate the performance of each bat’s solution. The algorithm then uses this fitness value to update the bats’ positions, velocities, loudness, and pulse rates, guiding the search towards better solutions. The goal of the BA is to find the optimal or near-optimal set of hyper-parameters that maximizes the performance of the SkewPNNs on the given classification task. By iteratively evaluating and updating the fitness of the candidate solutions, the BA efficiently searches the solution space, eventually converging to a set of hyper-parameters that yields improved classification accuracy and robustness, especially on imbalanced datasets. The fitness function’s design and choice of performance metrics are critical considerations, as they directly influence the success of the optimization process and the final performance of the SkewPNNs on the classification task.

3.3. Implementations of Proposed Algorithms

The structure of the proposed models is illustrated in Fig. 1a. To gauge the models’ efficacy, a rigorous evaluation was conducted employing the 10-fold cross-validation technique. This approach partitions the dataset into ten subsets, utilizing nine subsets for training and one for validation in each iteration. Such an approach offers a robust assessment by reducing the risk of overfitting and enhancing generalization because the model is trained and validated across diverse segments of the data, maximizing the utilization of available information. The training and testing datasets undergo normalization through z-score normalization. Subsequently, SkewPNNs are executed, with the notable modification of substituting the Gaussian kernel with the skew normal kernel within the proposed framework. The estimation of hyper-parameters is facilitated by the Bat Algorithm, which integrates a unique fitness function encompassing the maximization of the summation of accuracy, AUC-ROC, and F1-score. The flow chart of the proposed BA-SkewPNNs is shown in Fig. 1b. We delved into diverse configurations of the model’s pattern layer. Within this stratum, the PDF of each class is computed to ascertain the probability of an input instance’s association with each class. For every PDF, hyper-parameters are derived via two distinct methodologies, applied to both the Gaussian and the skew normal kernels. In the former approach, the hyper-parameters maintain uniformity across all patterns in the pattern layer. In the latter approach, however, the hyper-parameters vary for each pattern. In this context, the utilization of a population-based heuristic algorithm significantly aids in calculating distinct values for different patterns.

In this context, the employment of a population-based heuristic algorithm proves notably beneficial for computing distinct values for different patterns. This is because such algorithms, like the bat optimization technique used in our study, possess the capability to systematically explore the parameter space, adapting to the unique characteristics of each pattern. By allowing hyper-parameters to vary individually, the algorithm optimizes their values in alignment with the specific requirements and complexities of each pattern, ultimately enhancing the model’s adaptability and performance.

3.4. Consistency

The Parzen window estimator [52] for the PDF is expressed in Eqn. (2). K represents the kernel function, which, in our case, is the skew normal distribution. Here, $h(n)$ approaches zero as the number of data points increases. It is chosen in a way that the width of the window decreases, allowing for more localized estimation, as the dataset size grows. The specific choice of $h(n)$ can

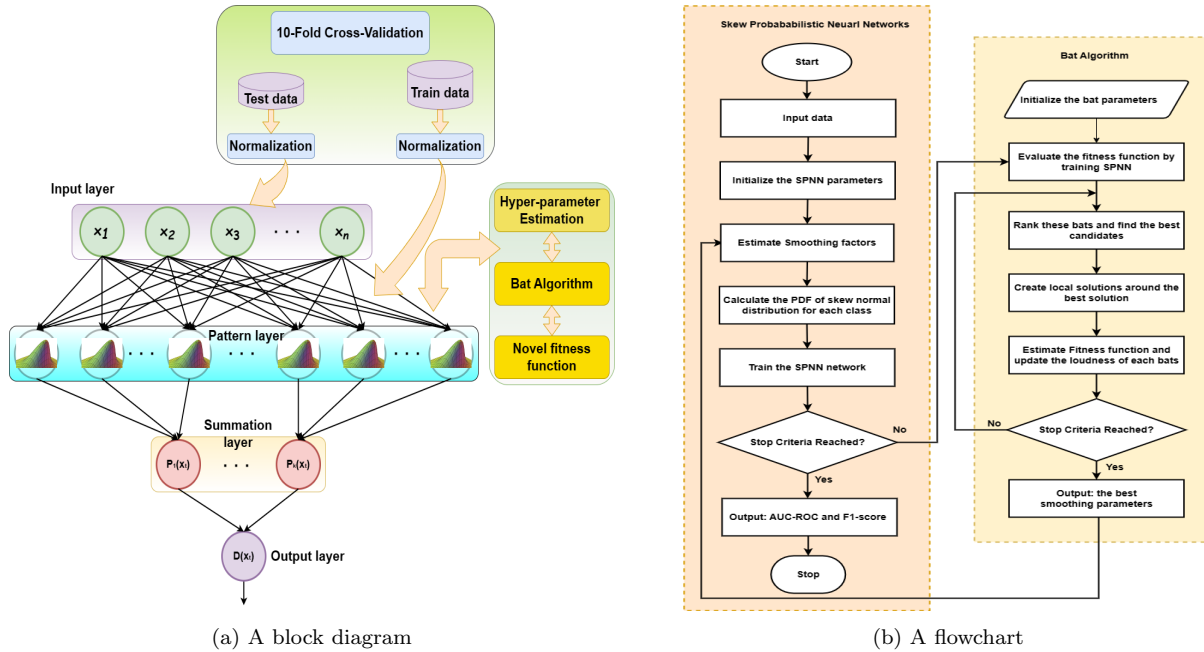


Figure 1: Skew Probabilistic Neural Networks: (a) Block diagram; (b) Flowchart of Bat algorithm-based SkewPNNs.

depend on the problem and the characteristics of the data. For simplicity, we will modify Eqn. (10) as given below

$$K(u; \alpha) = 2\phi(u)\Phi(\alpha u), \quad (11)$$

where, $x - x_i$ is represented as u for simplicity. The standard way to define consistency is that the expected error gets smaller as the estimates are based on a larger dataset. This is of particular interest since it will ensure that the true distribution will be approached in a smooth manner [52]. Conditions under which this happens for the density estimates are given by the following theorem:

Theorem 1. Suppose $K(x; \xi, \omega^2, \alpha)$ (as in Eqn. 9) is a Borel function satisfying the conditions:

- (A1) $\sup_{-\infty < x < \infty} |K(x; \xi, \omega^2, \alpha)| < \infty$,
- (A2) $\int_{-\infty}^{\infty} |K(x; \xi, \omega^2, \alpha)| dx < \infty$,
- (A3) $\lim_{x \rightarrow \infty} |xK(x; \xi, \omega^2, \alpha)| = 0$,
- (A4) $\int_{-\infty}^{\infty} K(x; \xi, \omega^2, \alpha) dx = 1$,

along with the conditions in Eqn. (2) and Eqn. (3), then the estimate $f_n(x)$ is consistent in quadratic mean in the sense that

$$\mathbb{E}|f_n(x) - g(x)| \rightarrow 0 \text{ as } n \rightarrow \infty.$$

Proof. To show that $K(x; \xi, \omega^2, \alpha)$ satisfying (A1) with skew normal kernel density, we need to find the mode of the skew normal distribution. For that, we establish the following result on log-concavity, that is, the logarithm of its density is a concave function.

Proposition 1. The distribution $K(x; \xi, \omega^2, \alpha)$ in SkewPNNs is log-concave.

Proof. It suffices to prove this for the case when $\xi = 0$ and $\omega^2 = 1$ since a change of location and scale do not alter the property. To prove that $\log K(x; \xi, \omega^2, \alpha)$ is a concave function of x , it is sufficient to show that the second derivative of $\log K(x; \xi, \omega^2, \alpha)$ is negative for all x , following [6]:

$$\frac{d^2}{dx^2} \log K(x; \xi, \omega^2, \alpha) = -1 + \frac{-\alpha^2 \phi(\alpha x)}{\Phi(\alpha x)} \left[\frac{\phi(\alpha x)}{\Phi(\alpha x)} + \alpha x \right]. \quad (12)$$

To show that the R.H.S. of Eqn. (12) is negative, it is sufficient to show that $B(\alpha x) = \left\{ \frac{\phi(\alpha x)}{\Phi(\alpha x)} + \alpha x \right\}$ is positive for all αx since $\phi(\alpha x)$ and $\Phi(\alpha x)$ are positive for all x .

Case I: If $\alpha x \geq 0$, then $B(\alpha x)$ is clearly positive.

Case II: If $\alpha x < 0$, let $v = -\alpha x$.

Then $\phi(\alpha x) = \phi(-\alpha x) = \phi(v)$ and $\Phi(\alpha x) = 1 - \Phi(-\alpha x) = 1 - \Phi(v)$. Therefore, we get

$$B(\alpha x) = \frac{\phi(v)}{1 - \Phi(v)} - v = r(v) - v,$$

where $r(v)$ is the failure rate of a standard normal random variable. Since it is known (see [4]) that $r(v) > v$ for all v , the assertion is proved. \square

Hence it is evident, that the mode is unique. An interesting observation for the $K(x; \xi, \omega^2, \alpha)$ is that the unimodality holds (univariate case) which coincides with the log-concavity of the distribution. We denote by $\xi + \omega m_0(\alpha)$ the mode of the skew normal distribution. For any general α , no explicit expression of $m_0(\alpha)$ is available and can be done using any iterative method such as Newton-Raphson numerical optimization method. However, the authors in [6] obtained a simple and practically accurate approximation as given below:

$$m_0(\alpha) \approx \mu_z - \frac{\gamma_1 \sigma_z}{2} - \frac{\text{sgn}(\alpha)}{2} \exp\left(-\frac{2\pi}{|\alpha|}\right),$$

where $\mu_z = \sqrt{\frac{2}{\pi}}\delta$ and $\sigma_z = \sqrt{1 - \mu_z^2}$. In addition, the authors in [6] obtained via numerical simulation that the mode occurs at $\alpha \approx 1.548$, $\delta = 0.8399$, where its value is 0.5427. Therefore, the maximum value of the $K(x; \xi, \omega^2, \alpha)$ is finite.

(A2) and (A4) are trivially satisfied as $K(x; \xi, \omega^2, \alpha)$ is a PDF of the skew normal distribution as defined in Eq. (9).

(A3) To show the limiting condition, we need the existence of the expectation.

$$\mathbb{E}_{K(x; \xi, \omega^2, \alpha)}[X] = \lim_{u \rightarrow \infty} \int_{-\infty}^u x K(x; \xi, \omega^2, \alpha) dx = \int_{-\infty}^{\infty} x K(x; \xi, \omega^2, \alpha) dx < \infty.$$

Since, [4] derived the expression for the mean of skew normal density function as follows: If $Y \sim SN(\xi, \omega^2, \alpha)$, then $\mathbb{E}[Y] = \xi + \omega \sqrt{\frac{2}{\pi}}\delta$, where $\delta = \frac{\alpha}{\sqrt{1 + \alpha^2}}$ for univariate case and it is well defined.

Now, for $u \geq 0$

$$\int_u^\infty xK(x; \xi, \omega^2, \alpha)dx \geq u \int_u^\infty K(x; \xi, \omega^2, \alpha)dx = u [1 - K_v(u; \xi, \omega^2, \alpha)],$$

where $K_v(u; \xi, \omega^2, \alpha)$ is the CDF of skew normal kernel used in SkewPNN. Therefore, it follows that

$$\lim_{u \rightarrow \infty} \left[\mathbb{E}_K [X] - \int_{-\infty}^u xK(x; \xi, \omega^2, \alpha)dx \right] = \lim_{u \rightarrow \infty} \int_u^\infty xK(x; \xi, \omega^2, \alpha)dx = 0$$

as in the limit, the term $\int_{-\infty}^u xK(x; \xi, \omega^2, \alpha)dx$ approaches to the expectation. By the inequality and the non-negativity of the integrand, we have the main result. Parzen [52] proved that the estimate $f_n(x)$ is consistent in quadratic mean if conditions (A1)-(A4) are met which satisfies in this case. \square

4. Experimental Results

4.1. Performance Measures

We consider the following two popularly used performance metrics for comparing state-of-the-art methods with our proposed models. The AUC-ROC serves as a critical metric for assessing the effectiveness of classifiers in distinguishing between positive and negative classes [38]. It visually illustrates the classifier’s performance by plotting *sensitivity* against $1 - \textit{specificity}$ at various thresholds, offering a consistent measure of the classifier’s ability to prioritize positive instances over negatives, regardless of the threshold used. Here, sensitivity, also referred to as recall, quantifies the proportion of actual positives correctly predicted by the classifier. In contrast, specificity measures the proportion of actual negatives correctly identified by the classifier. Precision denotes the ratio of true positive predictions to all predicted positives, while sensitivity measures the proportion of true positive predictions among actual positives as discussed in the previous subsection. The F1-score strikes a balance between precision and sensitivity, proving crucial in imbalanced dataset scenarios [55]. As the harmonic mean of precision and sensitivity, the F1-score succinctly evaluates classifier performance, ranging from 0 to 1. This metric is particularly valuable when achieving a trade-off between accurate identification and minimizing false positives is essential.

4.2. An Illustrative Example on Synthetic Spiral data

As an illustrative example, we utilize synthetic intertwined spiral datasets (two-class classification problems) from the `imbalanced-learn` library in Python [46]. These datasets contain two-dimensional points derived from a unique and complex pattern formed by the interplay of two spirals. The purpose of these examples is to demonstrate the distinct decision boundaries produced by various classifiers and their effectiveness in handling minority class instances. These datasets serve as valuable tools for visualizing the decision boundaries employed and for gauging the imbalance ratio accommodated by the SkewPNNs model. Throughout all experiments, 80% of the data samples are allocated for training, while the remainder is reserved for testing. For the simulated examples, we only compare the decision boundaries generated by our proposed method (we only consider Algorithm 1 in this context) with the most popularly used imbalanced learners. Here are the tuning parameters for each model: For HDDT, we set the maximum depth of the tree

to 5 for all examples. For the PNNs, we utilize a σ value of 0.1. Finally, our proposed model is applied to the datasets with σ value of 0.2 and α value of -2 for all synthetic examples. Fig. 2 shows a class imbalanced variant of the dataset with varying imbalance ratios. As illustrated in Fig. 2, our approach excels in accurately classifying minority samples, consistently achieving the highest F1-score values when compared to other classifiers across datasets with varying levels of class imbalance. This outcome reinforces the notion that our proposed approach is well-suited for handling highly imbalanced data structures.

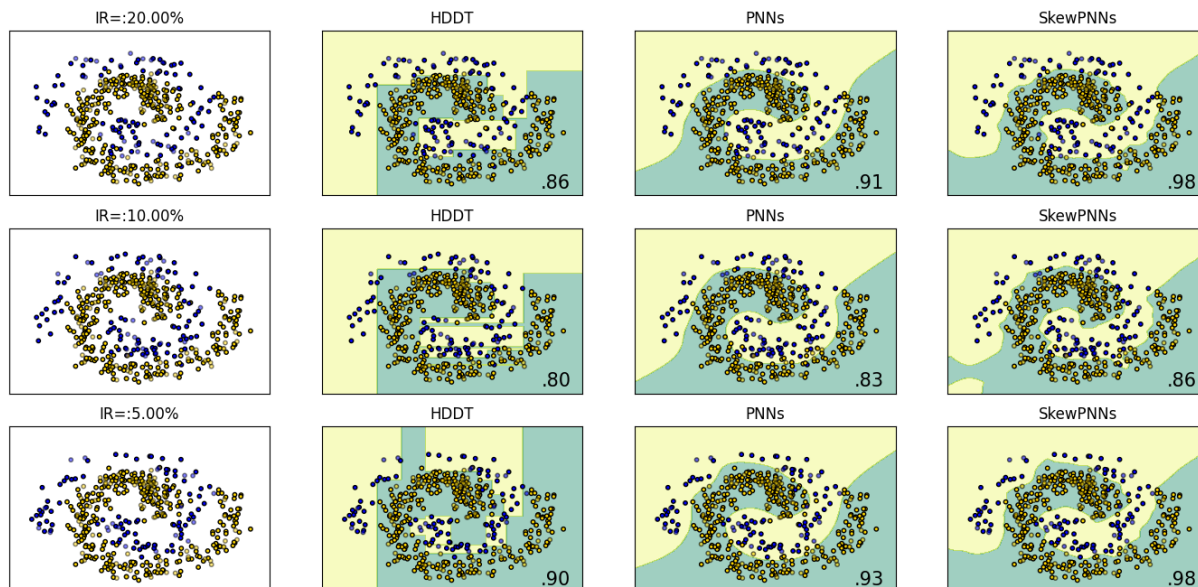


Figure 2: An illustrative evaluation (based on decision boundaries) of various classifiers for imbalanced datasets using synthetic data is presented. F1-scores are written in Black within the sub-figures.

4.3. Benchmark real-world datasets

Within imbalanced datasets, the imbalance ratio (IR) serves as a prevalent metric, quantifying the ratio between the sample size of the majority class and that of the minority class. In multiclass classification contexts, IR calculations account for the sample size of the largest majority class and the sample size of the smallest minority class. All the benchmark datasets are collected from open-source UCI and KEEL repositories. These imbalanced data challenges are commonly observed across a spectrum of real-world scenarios, encompassing datasets like Haberman, vehicle3, yeast, page, abalone, Ecoli, glass, etc. underscoring the need for specialized techniques to address these issues effectively. Likewise, we selected a subset of balanced datasets such as PIMA, tic-tac-toe, Bupa, hill valley, monks, etc. to evaluate the effectiveness of the proposed algorithm comprehensively. Further information on Imbalanced datasets (referred to as IDs) and the balanced datasets (referred to as BDs) along with IR are reported in Table 1.

Table 1: List of Imbalanced datasets and Balanced datasets utilized in experimentation.

Sr. No.	Datasets	#Samples	#Attributes	#Classes	IR	Sr. No.	Datasets	#Samples	#Attributes	#Classes	IR
ID1	Ecoli4	336	7	2	15.80	BD1	heart-c	1025	13	2	1.02
ID2	haberman	306	3	2	2.77	BD2	pima	768	8	2	1.86
ID3	vehicle3	846	18	2	2.99	BD3	tic-tac-toe	958	9	2	1.88
ID4	yeast-0-3-5-9 vs 7-8	506	8	2	9.12	BD4	australian	690	14	2	1.24
ID5	yeast-2 vs 4	514	8	2	9.07	BD5	bupa	345	6	2	1.37
ID6	page	5473	10	2	8.78	BD6	crx	690	15	2	1.24
ID7	abalone-20 vs 8-9-10	1916	8	2	72.69	BD7	ion	351	33	2	1.78
ID8	abalone9-18	731	8	2	16.40	BD8	hill valley	606	100	2	1.02
ID9	yeast4	1484	8	2	28.09	BD9	monks-2	432	6	2	1.11
ID10	Ecoli-0-2-3-4 vs 5	202	7	2	9.1	BD10	spect-f	80	44	2	1
ID11	glass-0-1-4-6 vs 2	205	9	2	11.05	BD11	wisconsin	683	9	2	1.85
ID12	car-good	1728	6	4	18.61						
ID13	car-vgood	1728	6	2	25.58						
ID14	dermatology-6	358	34	6	2.31						
ID15	flare-F	1066	11	6	7.69						
ID16	appendicitis	106	7	2	4.07						
ID17	transfusion	748	5	2	3.20						
ID18	lipid-indian-liver	583	9	2	2.49						

4.4. Analysis of Real-world Imbalanced and Balanced datasets

To assess the efficacy of the proposed SkewPNNs and BA-SkewPNNs, we implemented them on datasets characterized by balanced and imbalanced data distributions, as detailed in Table 1. Through a series of meticulously designed experiments on these standardized datasets, we systematically compared the performance of our method against a comprehensive array of techniques for class imbalanced (also balanced) learning, as outlined in Table 4. Our methodology commenced with the random shuffling of observations within each dataset, followed by the application of z-score normalization to ensure uniformity. Subsequently, we conducted rigorous 10-fold cross-validation, employing distinct and randomly generated training and test sets for each iteration. Moreover, our assessment encompassed a comprehensive comparative analysis between our proposed classifier, including its variations, and a range of established classifiers, which were employed as baseline benchmarks. This rigorous evaluation allowed us to conduct an in-depth examination of performance using key metrics such as AUC-ROC and F1-score.

Table 2: List of classifiers utilized in experimental evaluation.

Sr. No.	Classification Algorithms	Abbreviation
1	Decision Tree [42]	DT
2	Neural Network [54]	NN
3	Ada Boost [39]	AB
4	Random forest [11]	RF
5	SMOTE+ CART [12]	SC
6	SVR Tree [79]	SVR
7	Hellinger Distance Decision Tree [22]	HDDT
8	Hellinger Distance Random Forest [61]	HDRF
9	XG Boost [20]	XGB
10	Imbalanced XG Boost [63]	IXGB
11	Hellinger Net [16]	HN
12	Classical PNNs [59]	PNNs
13	Bat Algorithm based PNNs [69]	BA-PNNs
14	Skew normal PNNs (Proposed)	SkewPNNs
15	Bat Algorithm based Skew normal PNNs (Proposed)	BA-SkewPNNs

For the existing benchmark methods, we followed the standard implementation with the default setting parameters as done in the references mentioned in Table 2. To implement the conventional PNNs where the Gaussian kernel is employed, the smoothing parameter (σ) was systematically varied across the range of 0.01 or 0.1 till approximate constant (either 1 or 10), with increments of 0.05 or 0.1 for all samples. Subsequently, we explored an alternative approach. In this variant, we

integrated the Bat algorithm to dynamically assign optimal and distinct smoothing parameters for each sample during the PDF calculations. This model, denoted as BA-PNNs, operated with two distinct smoothing parameter intervals: $[0.01, 1.0)$ and $[0.1, 1.0)$. Moving forward, we conducted experiments utilizing our proposed SkewPNNs and BA-SkewPNNs. In the SkewPNNs, we leveraged the skew normal distribution for estimating the PDF values within pattern layers. Similarly, the smoothing parameter is chosen uniformly across samples, ranging from 0.01 or 0.1 to approximate constant (either 1 or 10), with intervals of 0.05 or 0.1. In case of the BA-SkewPNNs model, the BA algorithm was employed to assign the optimal and diverse smoothing parameters for the PDF calculations across all the samples. Likewise, two distinct intervals were maintained for selecting smoothing parameters: $[0.01, 1.0)$ or $[0.1, 1.0)$. Notably, the fitness function remained consistent for both BA-PNNs and BA-SkewPNNs.

Table 3: Experimental results encompassing AUC-ROC and F1-score analyses conducted on imbalanced datasets listed in Table 1. The highest value for a particular dataset is highlighted in bold.

Dataset	Measure	DT	NN	AB	RF	SC	SVR	HDDT	HDRF	XGB	IXGB	HN	PNNs	BA-PNNs	SkewPNNs	BA-SkewPNNs
ID1	AUC-ROC	0.819	0.859	0.818	0.820	0.765	0.802	0.787	0.803	0.943	0.968	0.900	0.908	0.921	0.933	0.980
	F1-score	0.622	0.756	0.716	0.726	0.612	0.621	0.601	0.700	0.526	0.893	0.889	0.744	0.857	0.774	0.881
ID2	AUC-ROC	0.540	0.579	0.594	0.555	0.582	0.638	0.552	0.546	0.548	0.513	0.550	0.588	0.595	0.588	0.665
	F1-score	0.312	0.304	0.353	0.300	0.310	0.478	0.332	0.275	0.308	0.244	0.294	0.402	0.401	0.403	0.513
ID3	AUC-ROC	0.667	0.598	0.637	0.637	0.629	0.711	0.685	0.666	0.666	0.648	0.662	0.709	0.712	0.711	0.718
	F1-score	0.499	0.344	0.438	0.433	0.396	0.547	0.528	0.490	0.491	0.463	0.488	0.548	0.558	0.551	0.561
ID4	AUC-ROC	0.599	0.598	0.659	0.539	0.549	0.648	0.652	0.588	0.623	0.536	0.568	0.676	0.741	0.718	0.751
	F1-score	0.286	0.279	0.401	0.129	0.153	0.345	0.369	0.256	0.333	0.138	0.235	0.331	0.455	0.449	0.449
ID5	AUC-ROC	0.795	0.821	0.841	0.830	0.801	0.869	0.819	0.832	0.825	0.826	0.833	0.902	0.902	0.896	0.910
	F1-score	0.625	0.741	0.729	0.749	0.642	0.703	0.672	0.750	0.609	0.696	0.667	0.779	0.776	0.745	0.776
ID6	AUC-ROC	0.904	0.923	0.879	0.919	0.914	0.911	0.912	0.925	0.878	0.922	0.934	0.851	0.903	0.850	0.912
	F1-score	0.833	0.853	0.801	0.870	0.846	0.832	0.842	0.880	0.792	0.866	0.885	0.678	0.770	0.671	0.767
ID7	AUC-ROC	0.638	0.566	0.615	0.542	0.587	0.643	0.597	0.525	0.793	0.586	0.600	0.791	0.809	0.812	0.842
	F1-score	0.283	0.180	0.283	0.117	0.201	0.253	0.190	0.067	0.400	0.266	0.333	0.121	0.191	0.130	0.231
ID8	AUC-ROC	0.605	0.592	0.657	0.534	0.597	0.655	0.615	0.557	0.560	0.558	0.562	0.660	0.689	0.691	0.719
	F1-score	0.264	0.284	0.420	0.113	0.242	0.308	0.256	0.187	0.200	0.206	0.222	0.207	0.282	0.301	0.362
ID9	AUC-ROC	0.670	0.538	0.595	0.557	0.589	0.672	0.641	0.574	0.554	0.562	0.565	0.846	0.853	0.847	0.861
	F1-score	0.352	0.120	0.234	0.179	0.189	0.304	0.289	0.202	0.154	0.212	0.222	0.305	0.337	0.334	0.346
ID10	AUC-ROC	0.836	0.892	0.869	0.845	0.825	0.839	0.845	0.845	0.958	0.976	1.000	0.908	0.934	0.913	0.930
	F1-score	0.683	0.813	0.767	0.730	0.677	0.697	0.730	0.730	0.960	0.945	1.000	0.733	0.834	0.743	0.821
ID11	AUC-ROC	0.554	0.500	0.687	0.547	0.536	0.610	0.704	0.522	0.469	0.575	0.813	0.642	0.757	0.745	0.747
	F1-score	0.167	0.000	0.417	0.133	0.111	0.278	0.440	0.067	0.050	0.210	0.571	0.196	0.270	0.264	0.280
ID12	AUC-ROC	0.934	0.838	0.629	0.876	0.921	0.942	0.941	0.870	0.875	0.837	0.855	0.889	0.919	0.913	0.953
	F1-score	0.908	0.760	0.341	0.837	0.847	0.875	0.921	0.818	0.762	0.784	0.789	0.681	0.704	0.716	0.720
ID13	AUC-ROC	0.991	0.843	0.951	0.968	0.970	0.977	0.983	0.984	0.775	0.939	0.906	0.917	0.958	0.958	0.983
	F1-score	0.983	0.769	0.885	0.949	0.947	0.956	0.966	0.976	0.600	0.931	0.897	0.635	0.771	0.635	0.760
ID14	AUC-ROC	0.949	1.000	0.999	1.000	0.959	0.978	0.999	0.975	0.812	0.954	1.000	1.000	1.000	1.000	1.000
	F1-score	0.913	1.000	0.980	1.000	0.926	0.955	0.980	0.967	0.769	0.950	1.000	1.000	1.000	1.000	1.000
ID15	AUC-ROC	0.637	0.555	0.531	0.556	0.516	0.698	0.649	0.569	0.619	0.546	0.581	1.000	1.000	1.000	1.000
	F1-score	0.201	0.146	0.092	0.126	0.041	0.242	0.218	0.145	0.261	0.144	0.222	1.000	1.000	1.000	1.000
ID16	AUC-ROC	0.698	0.764	0.692	0.703	0.721	0.704	0.659	0.747	0.691	0.710	0.639	0.801	0.811	0.791	0.826
	F1-score	0.507	0.600	0.492	0.490	0.546	0.512	0.398	0.597	0.467	0.467	0.462	0.667	0.692	0.614	0.698
ID17	AUC-ROC	0.638	0.573	0.629	0.599	0.556	0.640	0.619	0.605	0.605	0.610	0.561	0.602	0.650	0.610	0.672
	F1-score	0.448	0.267	0.413	0.378	0.175	0.455	0.419	0.386	0.380	0.384	0.313	0.399	0.464	0.408	0.451
ID18	AUC-ROC	0.573	0.500	0.573	0.563	0.503	0.539	0.598	0.598	0.590	0.567	0.526	0.660	0.660	0.676	0.669
	F1-score	0.377	0.000	0.355	0.330	0.831	0.813	0.429	0.394	0.386	0.353	0.308	0.682	0.651	0.642	0.687

The experimental findings for our proposed methodologies along with various existing methods detailed in Table 2 have been summarized in Tables 3 and 4. Table 3 particularly focuses on AUC-ROC and F1-score analyses conducted on the imbalanced datasets listed in Table 1. Note that we have accentuated the highest value for each specific dataset by highlighting it in bold, underscoring its significance. Among the 18 imbalanced datasets, fourteen showcase the highest AUC-ROC values, as indicated in Table 3. The Hellinger Net classifier emerges as the second-highest contributor to the number of highlighted highest AUC-ROC values. Notably, for the dermatology-6 and flare-F datasets, the AUC-ROC values are observed to be 100%, signifying excellent performance in cases of conventional PNNs, BA-PNNs, SkewPNNs, and BA-SkewPNNs. Upon comprehensive review of

Table 4: Experimental results encompassing AUC-ROC and F1-score analyses conducted on balanced datasets listed in Table 1. The highest value for a particular dataset is highlighted in bold.

Dataset	Measure	DT	NN	AB	RF	SC	SVR	HDDT	HDRF	XGB	IXGB	HN	PNNs	BA-PNNs	SkewPNNs	BA-SkewPNNs
BD1	AUC-ROC	0.725	0.827	0.791	0.795	0.498	0.524	0.733	0.81	0.814	0.795	0.607	1.000	1.000	1.000	1.000
	F1-score	0.705	0.811	0.766	0.770	0.044	0.212	0.709	0.788	0.798	0.775	0.525	1.000	1.000	1.000	1.000
BD2	AUC-ROC	0.690	0.728	0.735	0.704	0.699	0.703	0.679	0.712	0.714	0.718	0.688	0.724	0.727	0.716	0.737
	F1-score	0.594	0.639	0.650	0.605	0.600	0.627	0.584	0.617	0.627	0.627	0.582	0.645	0.634	0.645	0.650
BD3	AUC-ROC	0.882	0.840	0.660	0.923	0.850	0.790	0.896	0.925	0.998	0.918	0.799	0.796	0.711	0.812	0.775
	F1-score	0.924	0.905	0.803	0.959	0.800	0.730	0.929	0.960	0.999	0.955	0.863	0.814	0.761	0.835	0.773
BD4	AUC-ROC	0.797	0.867	0.867	0.858	0.850	0.812	0.798	0.860	0.856	0.851	0.774	0.631	0.669	0.532	0.859
	F1-score	0.776	0.854	0.853	0.842	0.834	0.799	0.775	0.843	0.839	0.835	0.755	0.557	0.529	0.421	0.858
BD5	AUC-ROC	0.597	0.688	0.683	0.685	0.619	0.616	0.597	0.695	0.704	0.705	0.607	0.634	0.688	0.635	0.688
	F1-score	0.664	0.767	0.746	0.736	0.549	0.538	0.670	0.754	0.759	0.769	0.680	0.575	0.643	0.599	0.644
BD6	AUC-ROC	0.821	0.864	0.857	0.864	0.846	0.797	0.812	0.880	0.883	0.865	0.799	0.632	0.796	0.634	0.864
	F1-score	0.805	0.853	0.843	0.848	0.861	0.837	0.792	0.868	0.873	0.852	0.767	0.548	0.790	0.549	0.862
BD7	AUC-ROC	0.843	0.913	0.900	0.925	0.877	0.871	0.846	0.924	0.920	0.891	0.879	0.942	0.928	0.942	0.934
	F1-score	0.895	0.951	0.935	0.950	0.843	0.833	0.895	0.955	0.953	0.935	0.909	0.953	0.949	0.953	0.945
BD8	AUC-ROC	0.546	0.500	0.481	0.581	0.536	0.509	0.508	0.580	0.601	0.535	0.532	0.527	0.523	0.526	0.533
	F1-score	0.582	0.000	0.549	0.576	0.697	0.567	0.499	0.593	0.602	0.541	0.496	0.388	0.554	0.381	0.459
BD9	AUC-ROC	0.764	0.517	0.488	0.631	0.489	0.485	0.754	0.618	0.736	0.651	0.583	0.982	0.821	0.984	0.866
	F1-score	0.704	0.136	0.245	0.512	0.346	0.302	0.688	0.483	0.680	0.556	0.500	0.981	0.839	0.981	0.885
BD10	AUC-ROC	0.642	0.512	0.690	0.643	0.543	0.618	0.647	0.661	0.629	0.627	0.747	0.763	0.750	0.763	0.764
	F1-score	0.855	0.045	0.878	0.882	0.148	0.385	0.849	0.888	0.874	0.863	0.889	0.725	0.647	0.666	0.671
BD11	AUC-ROC	0.947	0.965	0.953	0.959	0.944	0.949	0.944	0.964	0.944	0.962	0.961	0.963	0.960	0.967	0.970
	F1-score	0.932	0.952	0.941	0.947	0.926	0.928	0.927	0.952	0.933	0.950	0.950	0.966	0.972	0.976	0.979

the table, it is evident that the proposed SkewPNNs and BA-SkewPNNs demonstrate commendable performance. In a similar vein, we conducted an in-depth F1-score analysis on the imbalanced datasets detailed in Table 1, and the results are summarized in Table 3. This evaluation provides valuable insights into the performance of different classifiers. Upon careful examination of Table 3, it is evident that our proposed BA-SkewPNNs classifier boasts the highest number of highlighted F1-score values. Following closely, three different classifiers, namely Hellinger Net, PNNs, and BA-PNNs, also secure commendable rankings.

Furthermore, we conducted an AUC-ROC analysis on the balanced datasets delineated in Table 1. The results of this analysis are summarized in Table 4. Mirroring our approach with imbalanced datasets, we have highlighted the highest AUC-ROC values for better emphasis. Upon inspecting Table 4, we observe that out of the 11 datasets, eight stand out for their excellence in the case of our proposed BA-SkewPNNs method. Following closely, our proposed SkewPNNs also perform remarkably. Note that for the balanced heart-c dataset, AUC-ROC values reach a perfect 100%, signaling exceptional performance across conventional PNNs, BA-PNNs, SkewPNNs, and BA-SkewPNNs. In essence, our proposed methods consistently demonstrate superior performance, even in the context of balanced datasets. Similarly, we extended our F1-score analysis to the balanced datasets outlined in Table 1, with the results tabulated in Table 4. Here, once again, the BA-SkewPNNs demonstrate exceptional performance by securing the highest highlighted values for four out of the 11 datasets. Remarkably, for the balanced heart-c dataset, conventional PNNs, BA-PNNs, Skew-PNNs, and BA-SkewPNNs achieve a perfect F1-score of 100%. In summary, our proposed methodologies consistently outshine other classifiers, proving their mettle in both imbalanced and balanced dataset scenarios, particularly in terms of F1-score performance.

4.5. Statistical Test for Comparison of Classifiers

To gauge the statistical significance of our comparative methods, we conducted a Wilcoxon signed-rank test [67]. This non-parametric statistical assessment is tailored for comparing paired samples, aiming to discern if there exists a notable distinction between the associated observations. In our specific inquiry, the Null Hypothesis posits that there is no substantial difference between

our BA-SkewPNNs model and the other comparative approaches. We elected a 95% confidence level, implying that we consider outcomes to be statistically significant if the p-value falls below 0.05. This indicates that our proposed model demonstrates distinct performance compared to the other methods. The findings of the Wilcoxon signed-rank test and the assessment of significance are detailed in Table 5. For imbalanced datasets, both SkewPNNs and BA-SkewPNNs outperformed state-of-the-art imbalanced learners and other benchmark machine learners by significant margins for the majority of real-data examples.

Table 5: The statistical test results, specifically the p-values, comparing the performance of BA-SkewPNNs against other comparative methods have been examined for both imbalanced and balanced datasets.

	Measures	DT	NN	AB	RF	SC	SVR	HDDT	HDRF	XGB	IXGB	HN	PNNs	BA-PNNs
Imbalanced	AUC-ROC	0.0000	0.0004	0.0000	0.0004	0.0000	0.0000	0.0004	0.0000	0.0000	0.0001	0.0012	0.0004	0.0021
	F1-scores	0.0003	0.0003	0.0000	0.0003	0.0001	0.0001	0.0000	0.0000	0.0000	0.0000	0.0004	0.0005	0.0004
Balanced	AUC-ROC	0.0134	0.0208	0.0017	0.0597	0.0061	0.0005	0.0134	0.1465	0.2163	0.0574	0.0012	0.1167	0.0033
	F1-scores	0.2163	0.0327	0.3078	0.3757	0.0681	0.0479	0.0942	0.6355	0.5417	0.3054	0.0681	0.2719	0.0995

5. Conclusion and Discussion

Imbalanced datasets pose complexities in machine learning and classification endeavors. This disparity can prompt models to favor the over-represented class, resulting in compromised performance of the minority class. This discrepancy becomes particularly crucial when the minority class holds pivotal insights or embodies infrequent yet pivotal occurrences. In classification scenarios, when class distribution is notably skewed with one class holding notably more samples (majority class) than others (minority class), the dataset is labeled as imbalanced. This study introduced a novel approach that leverages PNNs in tandem with the skew normal kernel to address challenges associated with imbalanced datasets. Through this integration, we harness the PNN’s unique capability to provide probabilistic outputs, allowing for a nuanced understanding of prediction confidence and adept handling of uncertainty. The incorporation of the skew normal distribution, renowned for its adaptability in handling imbalanced and non-symmetric data, markedly enhances the representation of underlying class densities. To optimize performance on imbalanced datasets, fine-tuning of hyperparameters is crucial, a task we undertake using the bat optimization algorithm. Our study demonstrates the statistical consistency of density estimates, indicating a smooth convergence to the true distribution with increasing sample size. Rigorous statistical analysis furnishes robust evidence of the methodology’s effectiveness and broad applicability. Furthermore, extensive simulations and real-world data examples comparing various machine learning models resoundingly affirm the effectiveness of the SkewPNNs approach on both balanced and imbalanced data. Since advanced deep learning models do not work well on tabular data, we did not consider them in this study [58]. Looking ahead, future research avenues could focus on working on imbalanced regression problems [71] where hard boundaries between classes do not exist. We can extend our current work to accommodate regression tasks that involve continuous and even infinite target values (e.g., age of different people based on their visual appearances in computer vision where age is a continuous target and can be highly imbalanced).

Code and Data Availability

To support reproducible research and for future extensions and comparison, we are making the code and the data publicly accessible at <https://github.com/7shraddha/SkewPNN>.

References

- [1] Abiodun, O.I., Jantan, A., Omolara, A.E., Dada, K.V., Umar, A.M., Linus, O.U., Arshad, H., Kazaure, A.A., Gana, U., Kiru, M.U., 2019. Comprehensive review of artificial neural network applications to pattern recognition. *IEEE access* 7, 158820–158846.
- [2] Akbani, R., Kwek, S., Japkowicz, N., 2004. Applying support vector machines to imbalanced datasets, in: *Machine Learning: ECML 2004: 15th European Conference on Machine Learning, Pisa, Italy, September 20-24, 2004. Proceedings* 15, Springer. pp. 39–50.
- [3] Arnold, B.C., Lin, G.D., 2004. Characterizations of the skew-normal and generalized chi distributions. *Sankhyā: The Indian Journal of Statistics* , 593–606.
- [4] Azzalini, A., 1985. A class of distributions which includes the normal ones. *Scandinavian journal of statistics* , 171–178.
- [5] Azzalini, A., 2005. The skew-normal distribution and related multivariate families. *Scandinavian journal of statistics* 32, 159–188.
- [6] Azzalini, A., 2013. *The skew-normal and related families. volume 3.* Cambridge University Press.
- [7] Azzalini, A., Capitanio, A., 1999. Statistical applications of the multivariate skew normal distribution. *Journal of the Royal Statistical Society: Series B (Statistical Methodology)* 61, 579–602.
- [8] Azzalini, A., Valle, A.D., 1996. The multivariate skew-normal distribution. *Biometrika* 83, 715–726.
- [9] Baesens, B., Höppner, S., Ortner, I., Verdonck, T., 2021. robrose: A robust approach for dealing with imbalanced data in fraud detection. *Statistical Methods & Applications* 30, 841–861.
- [10] Barua, S., Islam, M.M., Yao, X., Murase, K., 2012. Mwmote–majority weighted minority oversampling technique for imbalanced data set learning. *IEEE Transactions on knowledge and data engineering* 26, 405–425.
- [11] Biau, G., Scornet, E., 2016. A random forest guided tour. *Test* 25, 197–227.
- [12] Blagus, R., Lusa, L., 2013. Smote for high-dimensional class-imbalanced data. *BMC bioinformatics* 14, 1–16.
- [13] Boonchuay, K., Sinapiromsaran, K., Lursinsap, C., 2017. Decision tree induction based on minority entropy for the class imbalance problem. *Pattern Analysis and Applications* 20, 769–782.
- [14] Cano, A., Zafra, A., Ventura, S., 2013. Weighted data gravitation classification for standard and imbalanced data. *IEEE transactions on cybernetics* 43, 1672–1687.
- [15] Chaabane, I., Guermazi, R., Hammami, M., 2020. Enhancing techniques for learning decision trees from imbalanced data. *Advances in Data Analysis and Classification* 14, 677–745.
- [16] Chakraborty, T., Chakraborty, A.K., 2020a. Hellinger net: A hybrid imbalance learning model to improve software defect prediction. *IEEE Transactions on Reliability* 70, 481–494.
- [17] Chakraborty, T., Chakraborty, A.K., 2020b. Superensemble classifier for improving predictions in imbalanced datasets. *Communications in Statistics: Case Studies, Data Analysis and Applications* 6, 123–141.
- [18] Chakraborty, T., Reddy, U., Naik, S.M., Panja, M., Manvitha, B., 2023. Ten years of Generative Adversarial Nets (GANs): A survey of the state-of-the-art. *arXiv:2308.16316*.
- [19] Chawla, N.V., Lazarevic, A., Hall, L.O., Bowyer, K.W., 2003. Smoteboost: Improving prediction of the minority class in boosting, in: *Knowledge Discovery in Databases: PKDD 2003: 7th European Conference on Principles and Practice of Knowledge Discovery in Databases, Cavtat-Dubrovnik, Croatia, September 22-26, 2003. Proceedings* 7, Springer. pp. 107–119.

- [20] Chen, T., He, T., Benesty, M., Khotilovich, V., Tang, Y., Cho, H., Chen, K., Mitchell, R., Cano, I., Zhou, T., et al., 2015. Xgboost: extreme gradient boosting. R package version 0.4-2 1, 1–4.
- [21] Cieslak, D.A., Chawla, N.V., 2008. Learning decision trees for unbalanced data, in: Machine Learning and Knowledge Discovery in Databases: European Conference, ECML PKDD 2008, Antwerp, Belgium, September 15-19, 2008, Proceedings, Part I 19, Springer. pp. 241–256.
- [22] Cieslak, D.A., Hoens, T.R., Chawla, N.V., Kegelmeyer, W.P., 2012. Hellinger distance decision trees are robust and skew-insensitive. *Data Mining and Knowledge Discovery* 24, 136–158.
- [23] Daniels, Z., Metaxas, D., 2017. Addressing imbalance in multi-label classification using structured hellinger forests, in: Proceedings of the AAAI Conference on Artificial Intelligence.
- [24] Datta, S., Das, S., 2015. Near-bayesian support vector machines for imbalanced data classification with equal or unequal misclassification costs. *Neural Networks* 70, 39–52.
- [25] Duda, R.O., Hart, P.E., Stork, D.G., 1995. Pattern classification and scene analysis. ed: Wiley Interscience .
- [26] Elor, Y., Averbuch-Elor, H., 2022. To smote, or not to smote? arXiv preprint arXiv:2201.08528 .
- [27] Farquard, M.A.H., Bose, I., 2012. Preprocessing unbalanced data using support vector machine. *Decision Support Systems* 53, 226–233.
- [28] Farshidvard, A., Hooshmand, F., MirHassani, S., 2023. A novel two-phase clustering-based under-sampling method for imbalanced classification problems. *Expert Systems with Applications* 213, 119003.
- [29] Fernández, A., García, S., Galar, M., Prati, R.C., Krawczyk, B., Herrera, F., 2018a. Learning from imbalanced data sets. volume 10. Springer.
- [30] Fernández, A., Garcia, S., Herrera, F., Chawla, N.V., 2018b. Smote for learning from imbalanced data: progress and challenges, marking the 15-year anniversary. *Journal of artificial intelligence research* 61, 863–905.
- [31] Genton, M.G., 2005. Discussion of" the skew-normal". *Scandinavian Journal of Statistics* 32, 189–198.
- [32] Gong, P., Gao, J., Wang, L., 2022. A hybrid evolutionary under-sampling method for handling the class imbalance problem with overlap in credit classification. *Journal of Systems Science and Systems Engineering* 31, 728–752.
- [33] Grzyb, J., Klikowski, J., Woźniak, M., 2021. Hellinger distance weighted ensemble for imbalanced data stream classification. *Journal of Computational Science* 51, 101314.
- [34] Gu, Q., Tian, J., Li, X., Jiang, S., 2022. A novel random forest integrated model for imbalanced data classification problem. *Knowledge-Based Systems* 250, 109050.
- [35] Gupta, A.K., González-Farías, G., Dominguez-Molina, J.A., 2004a. A multivariate skew normal distribution. *Journal of multivariate analysis* 89, 181–190.
- [36] Gupta, A.K., Nguyen, T.T., Sanqui, J.A.T., 2004b. Characterization of the skew-normal distribution. *Annals of the Institute of Statistical Mathematics* 56, 351–360.
- [37] Han, H., Wang, W.Y., Mao, B.H., 2005. Borderline-smote: a new over-sampling method in imbalanced data sets learning, in: International conference on intelligent computing, Springer. pp. 878–887.
- [38] Hanley, J.A., McNeil, B.J., 1982. The meaning and use of the area under a receiver operating characteristic (roc) curve. *Radiology* 143, 29–36.
- [39] Hastie, T., Rosset, S., Zhu, J., Zou, H., 2009. Multi-class adaboost. *Statistics and its Interface* 2, 349–360.
- [40] He, H., Bai, Y., Garcia, E.A., Li, S., 2008. Adasyn: Adaptive synthetic sampling approach for imbalanced learning, in: 2008 IEEE international joint conference on neural networks (IEEE world congress on computational intelligence), Ieee. pp. 1322–1328.
- [41] He, H., Garcia, E.A., 2009. Learning from imbalanced data. *IEEE Transactions on knowledge and data engineering* 21, 1263–1284.
- [42] Kotsiantis, S.B., 2013. Decision trees: a recent overview. *Artificial Intelligence Review* 39, 261–283.

- [43] Koziarski, M., 2021. Csmoute: Combined synthetic oversampling and undersampling technique for imbalanced data classification, in: 2021 International Joint Conference on Neural Networks (IJCNN), IEEE. pp. 1–8.
- [44] Krawczyk, B., 2016. Learning from imbalanced data: open challenges and future directions. *Progress in Artificial Intelligence* 5, 221–232.
- [45] Kundu, D., 2014. Geometric skew normal distribution. *Sankhya B* 76, 167–189.
- [46] Lemaître, G., Nogueira, F., Aridas, C.K., 2017. Imbalanced-learn: A python toolbox to tackle the curse of imbalanced datasets in machine learning. *The Journal of Machine Learning Research* 18, 559–563.
- [47] Lyon, R.J., Brooke, J., Knowles, J.D., Stappers, B.W., 2014. Hellinger distance trees for imbalanced streams, in: 2014 22nd International conference on pattern recognition, IEEE. pp. 1969–1974.
- [48] Mao, K.Z., Tan, K.C., Ser, W., 2000. Probabilistic neural-network structure determination for pattern classification. *IEEE Transactions on neural networks* 11, 1009–1016.
- [49] Montana, D., 1992. A weighted probabilistic neural network, in: *Advances in Neural Information Processing Systems*, pp. 1110–1117.
- [50] Moosaei, H., Ganaie, M., Hladík, M., Tanveer, M., 2023. Inverse free reduced universum twin support vector machine for imbalanced data classification. *Neural Networks* 157, 125–135.
- [51] Naik, S.M., Jagannath, R.P.K., Kuppli, V., 2020. Bat algorithm-based weighted laplacian probabilistic neural network. *Neural Computing and Applications* 32, 1157–1171.
- [52] Parzen, E., 1962. On estimation of a probability density function and mode. *The annals of mathematical statistics* 33, 1065–1076.
- [53] Richard, M.D., Lippmann, R.P., 1991. Neural network classifiers estimate bayesian a posteriori probabilities. *Neural computation* 3, 461–483. doi:10.1162/neco.1991.3.4.461.
- [54] Ripley, B.D., 1994. Neural networks and related methods for classification. *Journal of the Royal Statistical Society: Series B (Methodological)* 56, 409–437.
- [55] Sajjadi, M.S., Bachem, O., Lucic, M., Bousquet, O., Gelly, S., 2018. Assessing generative models via precision and recall. *Advances in neural information processing systems* 31.
- [56] Sardari, S., Eftekhari, M., Afsari, F., 2017. Hesitant fuzzy decision tree approach for highly imbalanced data classification. *Applied Soft Computing* 61, 727–741.
- [57] Sari, A., Putri, A., Rustam, Z., Pandelaki, J., 2021. Preprocessing unbalanced data using support vector machine with method k-nearest neighbors for cerebral infarction classification, in: *Journal of Physics: Conference Series*, IOP Publishing. p. 012037.
- [58] Shwartz-Ziv, R., Armon, A., 2022. Tabular data: Deep learning is not all you need. *Information Fusion* 81, 84–90.
- [59] Specht, D.F., 1990a. Probabilistic neural networks. *Neural networks* 3, 109–118. doi:10.1016/0893-6080(90)90049-Q.
- [60] Specht, D.F., 1990b. Probabilistic neural networks and the polynomial adaline as complementary techniques for classification. *IEEE Transactions on Neural Networks* 1, 111–121. doi:10.1109/72.80210.
- [61] Su, C., Ju, S., Liu, Y., Yu, Z., 2015. Improving random forest and rotation forest for highly imbalanced datasets. *Intelligent Data Analysis* 19, 1409–1432.
- [62] Tahir, M.A., Kittler, J., Yan, F., 2012. Inverse random under sampling for class imbalance problem and its application to multi-label classification. *Pattern Recognition* 45, 3738–3750.
- [63] Wang, C., Deng, C., Wang, S., 2020. Imbalance-xgboost: leveraging weighted and focal losses for binary label-imbalanced classification with xgboost. *Pattern Recognition Letters* 136, 190–197.
- [64] Wang, Y., Sun, P., 2023. Kernel principle component analysis and random under sampling boost based fault diagnosis method and its application to a pressurized water reactor. *Nuclear Engineering and Design* 406, 112258.
- [65] Wang, Y., Xu, Y., 2023. A non-convex robust small sphere and large margin support vector machine for imbalanced data classification. *Neural Computing and Applications* 35, 3245–3261.

- [66] Wilson, D.L., 1972. Asymptotic properties of nearest neighbor rules using edited data. *IEEE Transactions on Systems, Man, and Cybernetics* , 408–421.
- [67] Woolson, R.F., 2007. Wilcoxon signed-rank test. *Wiley encyclopedia of clinical trials* , 1–3.
- [68] Xu, B., Wang, W., Yang, R., Han, Q., 2021. An improved unbalanced data classification method based on hybrid sampling approach, in: *2021 IEEE 4th International Conference on Big Data and Artificial Intelligence (BDAI)*, IEEE. pp. 125–129.
- [69] Yang, X., Chen, W., Li, A., Yang, C., Xie, Z., Dong, H., 2019. Ba-pnn-based methods for power transformer fault diagnosis. *Advanced engineering informatics* 39, 178–185.
- [70] Yang, X.S., 2010. A new metaheuristic bat-inspired algorithm, in: *Nature inspired cooperative strategies for optimization (NISCO)*. Springer, pp. 65–74.
- [71] Yang, Y., Zha, K., Chen, Y., Wang, H., Katabi, D., 2021. Delving into deep imbalanced regression, in: *International Conference on Machine Learning*, PMLR. pp. 11842–11851.
- [72] Yen, S.J., Lee, Y.S., 2009. Cluster-based under-sampling approaches for imbalanced data distributions. *Expert Systems with Applications* 36, 5718–5727.
- [73] Yi, J.H., Wang, J., Wang, G.G., 2016. Improved probabilistic neural networks with self-adaptive strategies for transformer fault diagnosis problem. *Advances in Mechanical Engineering* 8, 1–13. doi:10.1177/1687814015624832.
- [74] Yuan, X., Chen, S., Zhou, H., Sun, C., Yuwen, L., 2023. Chsmote: Convex hull-based synthetic minority oversampling technique for alleviating the class imbalance problem. *Information Sciences* 623, 324–341.
- [75] Zhang, G.P., 2000. Neural networks for classification: a survey. *IEEE Transactions on Systems, Man and Cybernetics, Part C (Applications and Reviews)* 30, 451–462. doi:10.1109/5326.897072.
- [76] Zhang, Y., Fang, X., Fan, W., Tang, W., Cai, J., Song, L., Zhang, C., 2018. Interaction between bdnf and tnfr- α genes in schizophrenia. *Psychoneuroendocrinology* 89, 1–6.
- [77] ZHANG, Y., LU, R., HUANG, J., GAO, D., 2019. Evolutionary-based ensemble under-sampling for imbalanced data, in: *2019 16th International Computer Conference on Wavelet Active Media Technology and Information Processing*, IEEE. pp. 212–216.
- [78] Zheng, M., Li, T., Sun, L., Wang, T., Jie, B., Yang, W., Tang, M., Lv, C., 2021. An automatic sampling ratio detection method based on genetic algorithm for imbalanced data classification. *Knowledge-Based Systems* 216, 106800.
- [79] Zhu, Y., Li, C., Dunson, D.B., 2021. Classification trees for imbalanced data: Surface-to-volume regularization. *Journal of the American Statistical Association* , 1–11.